Mineralocorticoid receptor blockade improved gut microbiota dysbiosis by reducing gut sympathetic tone in spontaneously hypertensive rats

Cristina González-Correa [a,b,1], Javier Moleón [a,b,1], Sofía Miñano [a,1], Iñaki Robles-Vera [c], Marta Toral [c,d], Natividad Martín-Morales [e], Francisco O'Valle [b,e], Manuel Sánchez [a,b,*], Manuel Gómez-Guzmán [a,b], Rosario Jiménez [a,b,d,*], Miguel Romero [a,b,2], Juan Duarte [a,b,d,2]

[a] Department of Pharmacology, School of Pharmacy and Center for Biomedical Research (CIBM), University of Granada, 18071 Granada, Spain
[b] Instituto de Investigación Biosanitaria de Granada, ibs.GRANADA, Granada, Spain
[c] Centro Nacional de Investigaciones Cardiovasculares (CNIC), Madrid 28029, Spain
[d] Ciber de Enfermedades Cardiovasculares (CIBERCV), Spain
[e] Department of Pathology, School of Medicine, University of Granada, Granada, Spain

ARTICLE INFO

ABSTRACT

Microbiota has a crucial role in the host blood pressure (BP) regulation. The present study analyzes whether the mineralocorticoid receptor antagonist spironolactone ameliorates the dysbiosic state in a genetic model of neurogenic hypertension. Twenty-week-old male Wistar Kyoto rats (WKY) and spontaneously hypertensive rats (SHR) were randomly allocated into three groups: untreated WKY, untreated SHR, and SHR treated with spironolactone for 5 weeks. Spironolactone restored the Firmicutes/Bacteroidetes proportion, and acetate-producing bacteria populations to WKY levels. Spironolactone reduced the percentage of intestinal aerobic bacteria. The amelioration of gut dysbiosis was linked to a reduction in the gut pathology, an enhanced colonic integrity, a reduced gut permeability and an attenuated sympathetic drive in the gut. Spironolactone was unable to reduce neuroinflammation and oxidative stress in the paraventricular nuclei in the hypothalamus. Spironolactone reduced the higher Th17 cells proportion in mesenteric lymph nodes and Th17 infiltration in aorta, improved aortic endothelial function and reduced systolic BP. This study demonstrates for the first time that spironolactone reduces gut dysbiosis in SHR. This effect could be related to its capability to improve gut integrity and pathology due to reduced sympathetic drive in the gut.

1. Introduction

Systemic arterial hypertension is the most crucial risk factor contributing to worldwide cardiovascular morbimortality that can be modified and controlled [1,2]. The exact reason behind elevated blood pressure (BP) cannot always be determined, and its detection is still challenging. Mounting evidence has suggested a role for altered gut microbiota in hypertension [3–6]. In addition to demonstrations of dysbiosis [3], fecal microbiota transplants from hypertensive human donors into germ-free mice [4] or spontaneously hypertensive rats

(SHR) into Wistar Kyoto (WKY) normotensive rats resulting in elevated BP and sympathetic activity [5,6] are key evidence for the modulatory capabilities of gut microbiota on BP regulation, although the regulatory mechanisms in BP have not been fully discovered yet. Recently, there has been discovered new evidence of a dysfunctional gut-brain axis in hypertension, involving neuroinflammation, [6–8] the sympathetic response in the gut and intestinal tyrosine hydroxylase and noradrenaline (NA) levels [5,6]. Interestingly, drugs such as minocycline [9,10] or mycophenolate [7] or exercise [8], which reduce neuroinflammation, improve gut microbiota dysbiosis.

The renin-angiotensin-aldosterone system (RAAS) plays a crucial part in the onset and maintenance of vascular disease and hypertension. Interestingly, angiotensin-converting enzyme inhibition with captopril [11] or angiotensin receptor blockade with losartan [12] decreased BP, altered gut microbiota, improved gut pathology and permeability, and reduced neuroinflammation in the SHR, showing the key role of RAAS controlling gut-brain axis in hypertension. Aldosterone is a steroid hormone that is critically involved in fluid and electrolyte balance as well as BP control through the mineralocorticoid receptor (MR) [13]. In addition, in the SHR forebrain, increased MR expression causes a bias towards a pro-inflammatory phenotype characteristic for hypertensive encephalopathy [14]. Previous studies [15–17] also demonstrated that MR blockade reduced BP as well as vascular dysfunction and hypertrophy in SHR. However, whether the MR antagonism reduces neuroinflammation in central nuclei involved in autonomic control of hypertension, such as the hypothalamic paraventricular nucleus (PVN), which participates in sympathetic outflow and regulates gut microbiota composition, is unclear. We hypothesized that MR antagonism might improve gut dysbiosis by reducing gut sympathetic tone as consequence of neuroinflammation reduction in SHR. Accordingly, we aimed to study the effects of spironolactone, a competitive aldosterone receptor antagonist used for over 40 years to treat diseases associated with primary or secondary hyperaldosteronism and resistant hypertension, in the gut microbiota composition and gut pathology and permeability in a genetic model of hypertension. SHR is a widely used animal model of sympathetic activation and neurogenic hypertension [18].

2. Materials and methods

2.1. Animals and experimental groups

All procedures in the present study were conducted in accordance with the European Union regulations and requirements on the protection of animals used for scientific purposes. The necessary protocol was approved by the Ethics Committee of Laboratory Animals of the University of Granada (Spain; permit number 16/02/2022/013/A). Animal studies follow the ARRIVE guidelines [19]. Twenty-weeks-old male SHR and WKY rats from Janvier Labs (Le Genest-Saint-Isle, Saint Berthevin Cedex, France) were used in the study. The animals were distributed into three groups: a) untreated WKY (WKY, 1 mL of vehicle (methylcellulose 1 %) day^{-1}, n = 8), b) untreated SHR (SHR, 1 mL of vehicle day^{-1}, n = 8), and c) and SHR treated with spironolactone (SHR-SPIR, 30 mg Kg^{-1} day^{-1} by gavage for 5 weeks, n = 8) [20]. Rats were housed in individual ventilated cages. Food and water intake were recorded daily. For the duration of the experiment, rats accessed to food and water ad libitum. Body weight was recorded weekly. Spironolactone treatment was stopped 48 h previous to the experimental endpoint, to better assess its long-term effects avoiding the possible masking of acute administration effects.

2.2. Blood pressure measurements

2 weeks were allowed for the rats to adapt at to vehicle administration, systolic blood pressure (SBP) and heart rate (HR) measurements were established before the procedural start. SBP and HR were obtained at room temperature in the morning, in no anesthetized, restrained rats

(prewarmed for 10–15 min at 35 °C) by tail-cuff plethysmography (LE 5001 Pressure Meter, Letica SA, Barcelona, Spain) as detailed in previous articles [21]. Briefly, animals were held in a plastic tube, and their tail was put through a rubber cuff, and the cuff was inflated with air. The pressure level at which the first pulse appeared, after blood flow had been interrupted with the inflated cuff, was designated SBP. At least 10 determinations were made in every session, and the mean of these values was taken as the SBP level.

2.3. Tissue collection and cardiac and renal weight indices

At procedural endpoint, the animals fasted overnight and were anesthetized with 2.5 mL/kg equitensin (i.p.) and exsanguinated through the abdominal aorta. The heart, kidney and brain tissues were rapidly removed and cleaned. The PVN tissues excised from frozen brain tissues as previously reported [22]. The heart was weighed, and then divided into the right ventricle and the left ventricle plus septum. The samples were immediately submerged in liquid nitrogen and later retrieved and kept at − 80ºC.

2.4. Histological evaluation of gut pathologies

At the end of the experiment, segments of colon were prepared for conventional morphology analysis, as previously described [8,23]. Briefly, samples were fixed in 10 % formalin buffered solution for 48 h and then transferred to 70 % ethanol. Paraffin embedded 4 μm sections were stained with hematoxylin-eosin (H&E), Masson-trichrome and Movat's pentachromic and observed under a BX42 light microscope (Olympus Optical Company, Ltd., Tokyo, Japan) with a 20x objective to visualize the general morphology and submucosal vascular-connective tissue. 10x images were also captured with a CD70 camera (Olympus Optical Company, Ltd.) attached to the microscope for the quantification of the thickness and area of submucosal fibrosis, thickness and area of the smooth muscle cell layer, number of goblet cells per 100 epithelial cells, crypt depth and the area of the submucosal vascular smooth muscle layer using ImageJ software (http://imagej.nih.gov/ij/). A double-blind evaluation was performed by experienced researchers (F. O. & N.M.-M.).

2.5. Plasma determinations

Blood samples kept on ice were centrifuged at 3500 rpm at 4ºC for 10 min to obtain plasma, which was frozen at − 80 °C. According to the manufacturer's instructions, the Amebocyte Lysate Chromogenic Endotoxin Quantitative Kit (Lonza, Valais, Switzerland) was utilized to determine lipopolysaccharide (LPS) levels in plasma. NA and intestinal fatty acid-binding protein 2 (I-FABP) in the plasma were measured using a noradrenaline ELISA kit (IBL International, Hamburg, Germany) and an I-FABP ELISA kit (R&D Systems, Minneapolis, MN), respectively, following the manufacturer's protocol.

2.6. Vascular reactivity studies

Samples from the descending aorta (3 mm) were placed in organ chambers with Krebs solution (in mmol/L: NaCl 118, NaHCO$_3$ 25, glucose 11, KCl 4.75, CaCl$_2$ 2, KH$_2$PO$_4$ 1.2, MgSO$_4$ 1.2) as detailed previously [24]. Concentration-contractile response curves to phenylephrine (10^{-9}-10^{-5} mol/L) were constructed in intact aortic rings from all experimental groups. The relaxation curves to acetylcholine (10^{-9} to 10^{-4} mol/L) were studied in phenylephrine pre-contracted ring-shaped samples (10 μmol/L). Additional curves were performed incubating with N^G-nitro-L-arginine methyl ester (L-NAME, a non-selective competitive inhibitor of nitric oxide synthase, 10^{-4} mol/L) or VAS2870 (non-selective inhibitor of NADPH oxidase, 5 μmol/L) for 30 min. Results were represented as a percentage of precontraction tension levels.

2.7. NADPH oxidase activity

As reported in other articles [25], we determined the NADPH oxidase activity in intact samples of aorta by a lucigenin-enhanced chemiluminescence assay. Segments of aorta from all groups were incubated at 37ºC for 30 min in a physiological salt solution (pH 7.4) with the following composition (in mmol/L): $CaCl_2$ 1.2, glucose 5.5, HEPES 20, KCl 4.6, KH_2PO_4 0.4, $MgSO_4$ 1, NaCl 119, $NaHCO_3$ 1 and Na_2HPO_4 0.15. Adding NADPH (100 µmol/L) and lucigenin (5 µmol/L). We measured the resulting luminescence for 200 s periods in 5-s intervals in a scintillation counter (Lumat LB 9507, Berthold, Germany) and determined enzyme activity by subtracting the basal values from the NADPH-treated values, expressing results as relative light units (RLU)/min/mg of tissue.

As performed in previous experiments [6], PVN NADPH oxidase activity was assessed in a microplate reader from tissue homogenates (10 µg protein) adding DHE (10 µmol/L) and deoxyribonucleic acid (DNA, 1.25 µg/mL) in PBS (100 mmol/L), pH 7.4, containing 100 µmol/L DTPA and NADPH (50 µmol/L) to a final volume of 120 µL, incubating for 30 min at 37ºC in the dark, in the absence or presence of apocynin, a NADPH oxidase inhibitor (50 µmol/L). The fluorescence was detected in a fluorescence spectrophotometer (Fluorostart, BMG Labtechnologies, Offenburg, Germany) using a rhodamine filter (excitation 490 nm, emission 590 nm) in a microplate reader. NADPH oxidase activity was calculated as difference of relative unit of fluorescence without and with apocynin and expressed a fold change respect WKY group.

2.8. Reactive oxygen species (ROS) concentrations in the PVN

PVN ROS levels were determined through the fluorescent probe 5-(and-6-) chloromethyl-2'− 7'-dichlorodihydrofluorescein diacetate (CM-H2DCFDA). The homogenates from 10 µg of protein were prepared in a non-denaturing lysis buffer (50 mmol/L Tris-HCl (pH 7.4) containing 10 µg/mL aprotinin, 0.1 mmol/L EDTA, 0.1 mmol/L EGTA, 10 µg/mL leupeptin and 1 mmol/L PMSF) and incubated in 96-well plates with 5 µmol/L CM-H2DCFDA for 30 min at 37 ºC. The fluorescence was detected in a spectrofluorimeter (Fluorostart, BMG Labtechnologies, Offenburg, German [6].

2.9. Flow cytometry

Mesenteric lymph nodes (MLN), blood and aortae were collected from all animals. These samples were adequately mashed with wet slides to reduce friction. Next, the red blood cells were lysed with Gey's solution and filtered through a 70 µM cell strainer. 1×10^6 cells were obtained and used per panel and organ. To improve the fluorescence signal for cytokines, we incubated our samples with 50 ng/mL PMA plus 1 µg/mL ionomycin for 30 min, then added a protein transport inhibitor (BD GolgiPlugTM) for 4 h at 37 °C. Next, the samples were pipetted into polystyrene tubes for staining. The cells were blocked with anti-CD32 (clone D34–485, BD Biosciences) to prevent non-specific bindings to Fc-gamma receptors, concomitantly, samples were incubated with a viability dye (LIVE/DIED® Fixable Aqua Dead cell Sain Kit, Molecular Probes, Oregon, USA) in PBS for 20 min at 4 °C in the dark. After washing with PBS, cells were stained for 30 min at 4ºC for surface targets with mAbs anti-CD4 (PerCP-Vio700, clone REA482, Miltenyi Biotec, Bergisch Gladbach, Germany), anti-CD45 (APC, clone RA3–6B2 BD PharmigenTM, New Jersey, USA), and anti-CD25 (PE-VIO770, clone 7D4, Miltenyi). The lymphocytes were then fixed and permeabilized simultaneously with the Fix/Perm Fixation/Permeabilization kit (eBioscience, San Diego, USA) and intracellular targets were stained with mAbs anti-IL-17A (PE-Cy7, clone eBio17B7, eBioscience, San Diego, USA), and anti-IFN-γ (PE-VIO770, clone XMG1.2, eBioscience, San Diego, USA) for 30 min at 4 °C in the dark. Samples were processed with a FACS ARIA III flow cytometer (BD Biosciences) and the analysis was performed with FlowJo software (Tree Star, Ashland, OR, USA) [26].

2.10. Gene and protein expression analysis

Colonic and PVN gene expression was carried out through quantitative polymerase chain reaction (qPCR), as stablished in previous experiments [25]. Hence, samples were homogenized to obtain RNA with TRI Reagent®. RNA concentration was assessed using a NanoDropTM 2000 Spectrophotometer (Thermo Fisher Scientific, Inc., Waltham, MA, USA). 2 µg of RNA from all samples were retrotranscribed into cDNA using oligo(dT) primers (Promega, Southampton, UK). The qPCR was performed using a Techne Techgene thermocycler (Techne, Cambridge, UK). The forward and reverse probes used for amplification are listed in (Table S1). A dilution series of standard vascular samples determined the efficiency of the reaction. We used GADPH expression for housekeeping normalization. The mRNA relative expression was determined using the ΔΔCt method.

We examined the content of zonula occludens protein-1 (ZO-1) and occludin in colonic homogenates by western blots. These samples were run on a sodium dodecyl sulphate-polyacrilamide electrophoresis (40 µg of protein per lane). Next, the transference of proteins was performed to polyvinylidene difluoride membranes. ZO-1 and occludin were detected after the membranes were incubated with the respective primary antibodies: rabbit polyclonal anti-occludin (Abcam, Cambridge, UK) and rabbit polyclonal anti-tight junction protein ZO-1 (Novus biological, Cambridge, UK). All were incubated at 1/1000 dilution overnight at 4ºC. The membranes were then incubated with secondary peroxidase-conjugated goat antirabbit (1/10000; Santa Cruz Biotechnology). Antibody binding was detected by a ECL system (Amersham Pharmacia Biotech, Amersham, UK) and densiometric analysis was done by ImageJ software. Samples were re-probed for smooth muscle α-actin.

2.11. DNA extraction, 16 S rRNA gene amplification, bioinformatics

For an analysis of intestinal microbial populations, we obtained faecal samples at the experimental endpoint. DNA was extracted from the samples using G-spin columns (INTRON Biotechnology) starting from 30 mg of faecal matter resuspended in PBS. RNAses and Proteinase K were utilized to treat all samples. Quant-IT PicoGreen reagent (Thermo Fischer) was used to quantify DNA concentrations. Then, we proceeded to the amplification of the V3-V4 regions for the 16 S rRNA gene [8] in all samples (about 3 ng). Extension tails present in the PCR products (approx. 450 pb) were used for barcoding and the addition of specific Illumina sequences in a low-cycle number PCR. Individual amplicon libraries were studied with the Bioanalyzer 2100 (Agilent) and a pool of samples was generated in equimolar concentrations. The pool was purified further and quantified; and the concentration determined through qPCR (Kapa Biosystems). Finally, the resulting DNA was sequenced on an Illumina MiSeq instrument with 2×300 paired-end read sequencing at the Unidad de Genómica (Parque Científico de Madrid, Spain).

BIPES pipeline was used to sort raw sequences. The barcode probes were trimmed and filtered if ambiguous bases or mismatches in the primer regions were detected as per the BIPES protocol. Sequences with more than one mismatch within the 40–70 bp region at each end were excluded. 30 Ns was used to concentrate the two single-ended sequences for the downstream sequence analyses. UCHIME (implemented in USEARCH, version 6.1) was conducted to screen out and remove chimeras in the de novo mode (using-minchunk 20-xn 7-noskipgaps 2). Additional analyses were carried out utilizing the 16 S Metagenomics (Version: 1.0.1.0) from Illumina. The sequences were clustered to an operational taxonomic unit (OTU) with USEARCH on default parameters (USERACH6.1). The threshold distance was set to 0.03. Thus, when the similarities between two 16 S rRNA sequences were over 97 %, the sequences were classified as the same OTU. QIIME-based alignments of representative sequences were conducted with PyNAST, and the SILVA database acted as template file. We utilized the Ribosome Database Project (RDP) algorithm representative sequences classification into
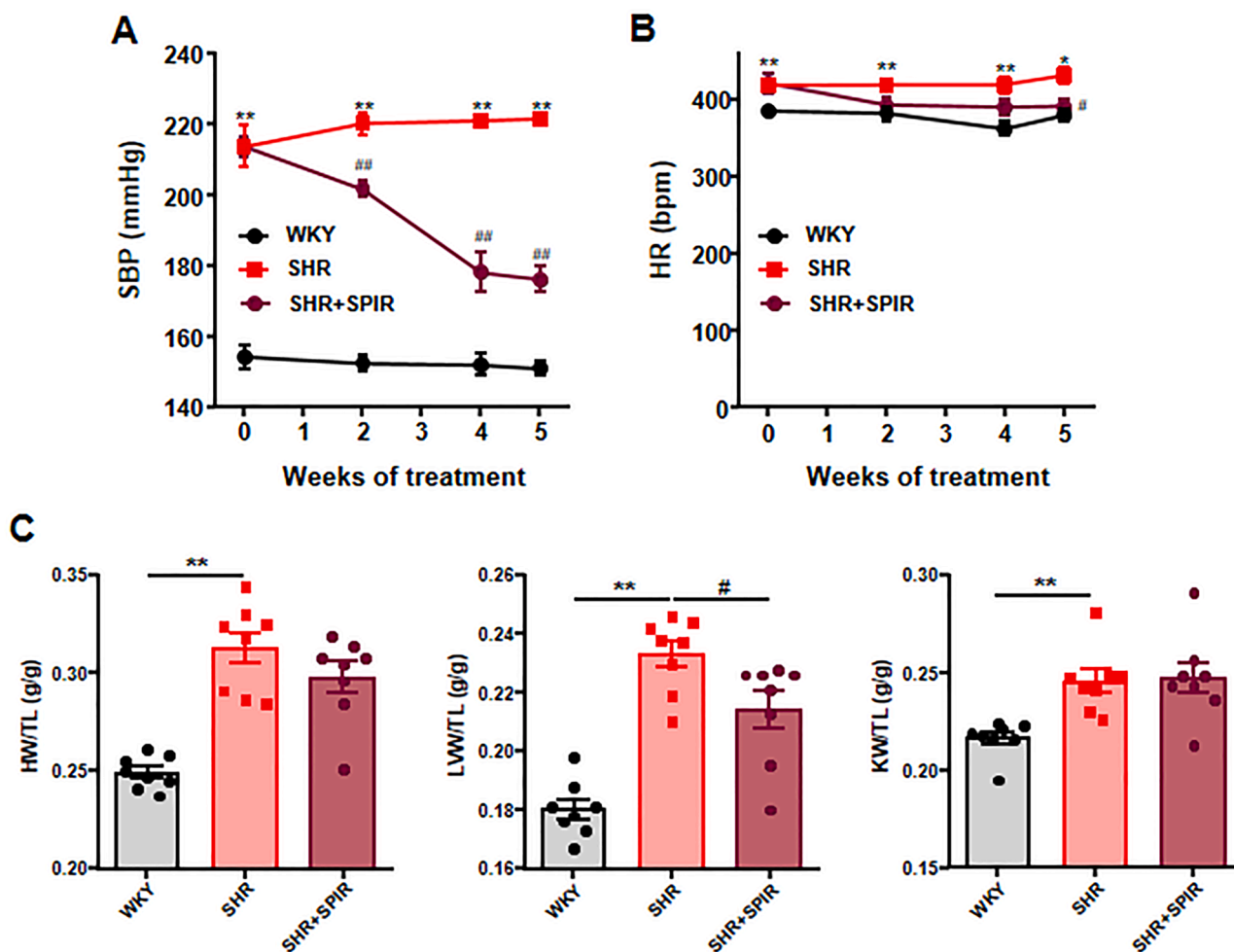
Fig. 1. Spironolactone (SPIR) reduces blood pressure and target organ damage in spontaneously hypertensive rats (SHR). Time course of systolic blood pressure (SBP) (A) and heart rate (HR) (B) measured by tail-cuff plethysmography. C) Ratio heart weight/tibia length (HW/TL), left ventricle weight/tibia length (LVW/TL), and kidney weight/tibia length (KW/TL). Values are expressed as mean ± SEM (n = 8). *P < 0.05 and * *P < 0.01 significant differences compared with Wistar Kyoto rats (WKY). $^{\#}$P < 0.05 and $^{\#\#}$P < 0.01 significant differences compared with untreated SHR group.

specific taxa with the default database. The Taxonomy Database (National Center for Biotechnology Information) was used for classification and nomenclature. Bacteria were classified based on short chain fatty acids (SCFAs) end-product, as previously described [8]. Briefly, genera were classified into more than one group if they were defined as producers of different metabolites. Bacteria were classified according to their oxygen requirements with the Genomes OnLine Database (GOLD) [8]. The obtained data were presented as relative abundance of predicted functions within the samples.

2.12. Reagents

All reagents were obtained from Merk (Barcelona, Spain) unless otherwise specified.

2.13. Statistical analysis

The Shannon and Chao Richness were calculated using the phyloseq package. Reads in each OTU were normalized to total reads in each sample. Only taxa with a prevalence in samples > 20 % and minimum count of 4 reads, and the data from minimum library size according to data rarefying were utilized for the analysis. Linear Discriminant Analyze (LDA) scores greater than 3.5 were displayed. Taxonomy was summarized at the genus level and uploaded to Microbiome Analyst [27] to generate LDA effect size (LEfSe) where significant enrichment

was considered at a P < 0.05, LDA score > 3.5. Results are expressed as means ± SEM of measurements. The non-parametric factorial Kruskal-Wallis sum-rank test was performed to identify features with significant differential abundance, followed by LDA to calculate the effect size of each differentially abundant features. Beta diversity analyses was carried out, comparing the changes in the presence/absence or abundance of thousands of taxa present in a dataset and summarize these into how 'similar' or 'dissimilar' two samples. Each sample gets compared to every other sample generating a distance or dissimilarity matrix. The Bray-Curtis distance was used to analyze beta diversity. The result is represented by Principal Coordinate Analysis (PCoA).

Tail SBP, HR and the concentration-response curves to phenylephrine and acetylcholine were analyzed by two-way repeated-measures ANOVA with the Bonferroni post hoc test. Other variables were tested for normal distribution using Shapiro-Wilk normality test and compared using one-way ANOVA and Tukey post hoc test in case of normal distribution or Mann–Whitney *U* test or Kruskal–Wallis with Dunn's multiple comparison test in case of abnormal distribution. P < 0.05 was considered statistically significant.
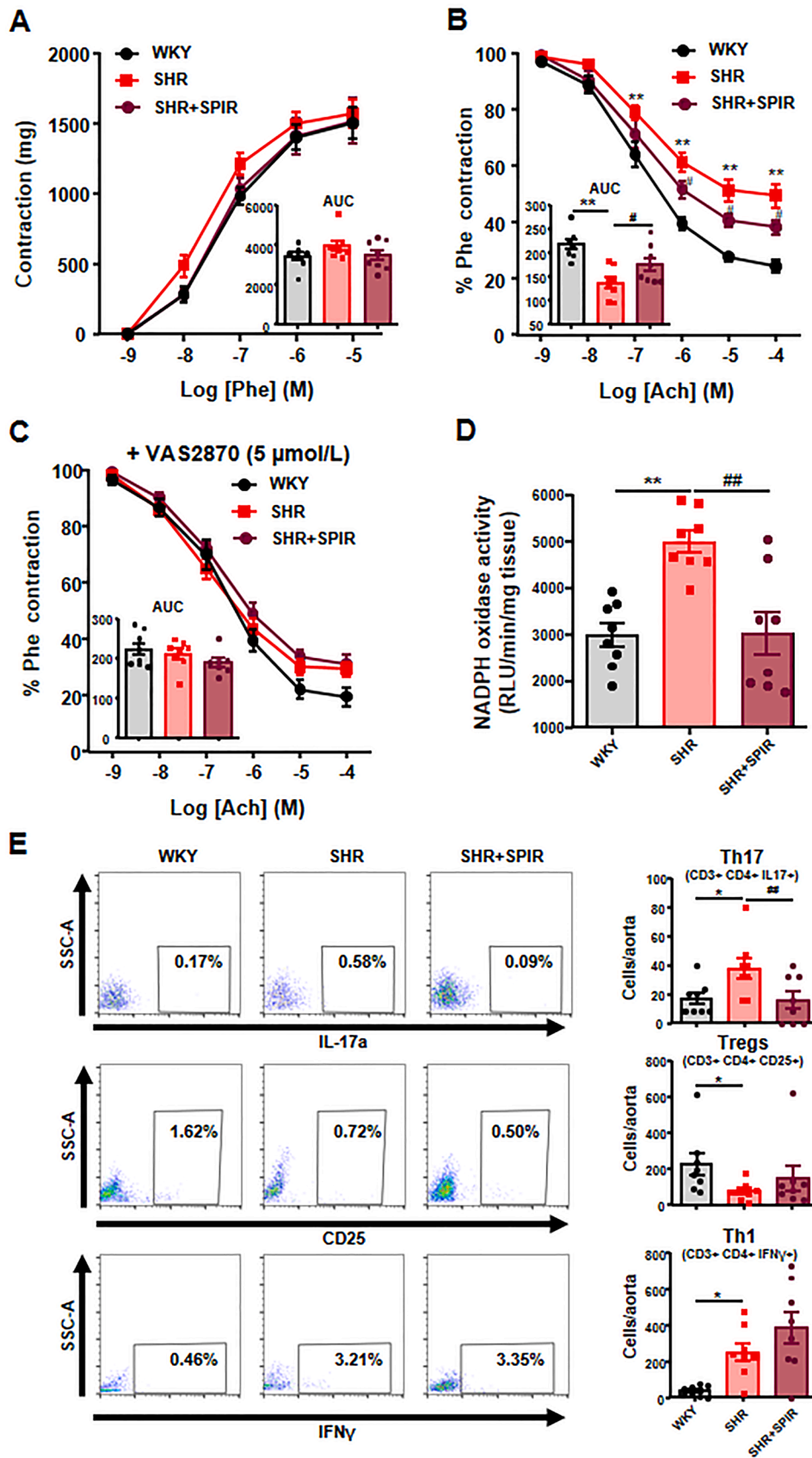
Fig. 2. Spironolactone (SPIR) improves endothelial dysfunction and Th17 infiltration in aorta from spontaneously hypertensive rats (SHR). **A)** Concentration-contractile response curve induced by phenylephrine (Phe). Endothelium-dependent relaxation induced by acetylcholine (Ach) in aortas precontracted by phenylephrine in the absence (B) or in the presence of VAS2870 (C). NADPH oxidase activity measured by chemiluminescence to lucigenin (D), and Th17, Tregs, and Th1 infiltration measured by flow cytometry (E) in aorta from all experimental groups. Values are expressed as mean ± SEM (n = 8). *P < 0.05 and * *P < 0.01 significant differences compared with Wistar Kyoto rats (WKY). #P < 0.05 and ##P < 0.01 significant differences compared with untreated SHR group. AUC: area under curve.
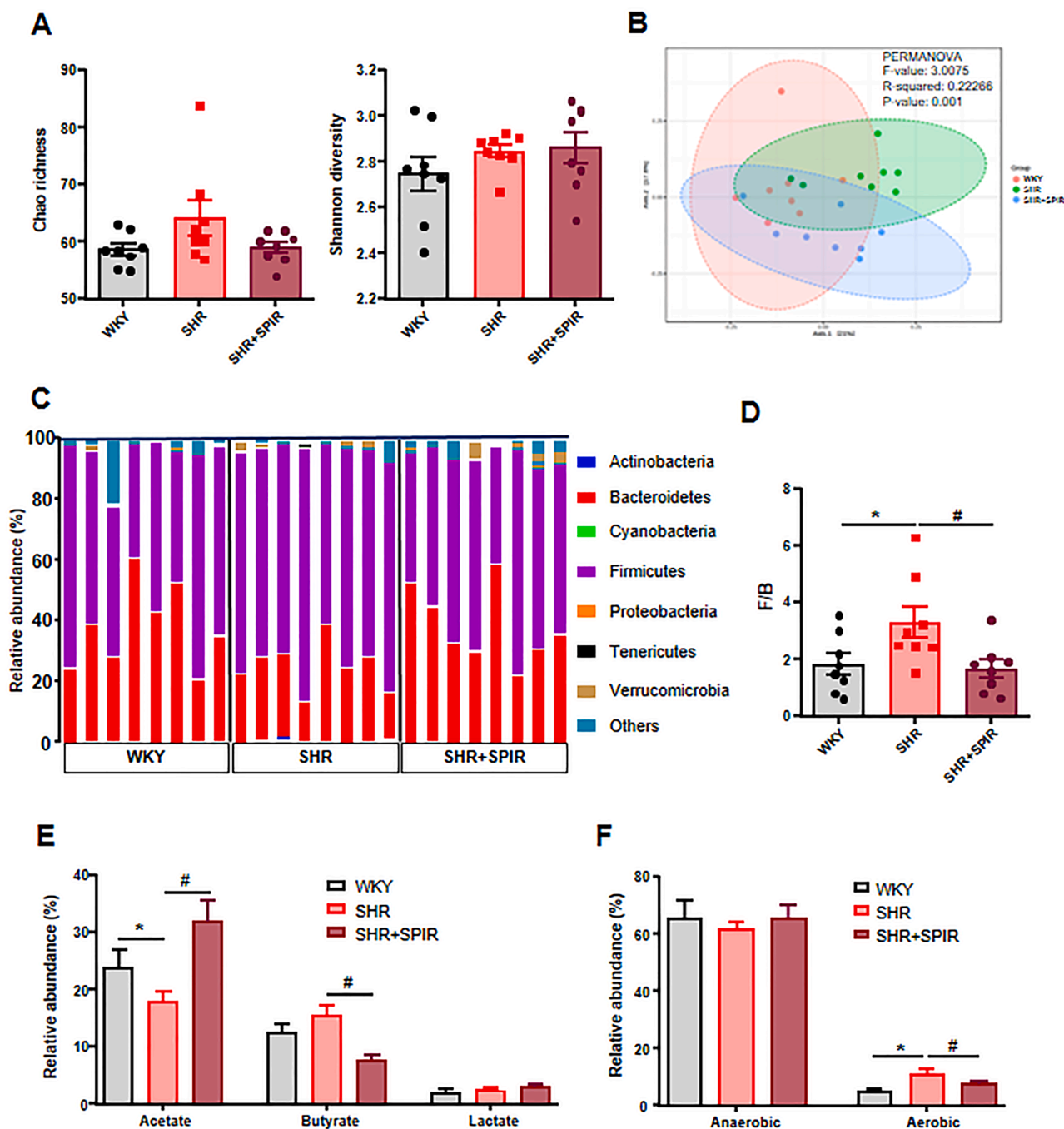
Fig. 3. Spironolactone (SPIR) reshapes the remodeling of gut microbiota in spontaneously hypertensive rats (SHR). The microbial DNA from fecal samples was analyzed by 16 S rRNA gene sequencing. A) Ecological parameters of richness, and diversity. B) Principal Coordinate Analysis (PCoA) in the gut microbiota from all experimental groups. C) Phylum breakdown of the seven most abundant bacterial communities in the faecal samples was obtained from all experimental groups. D) Firmicutes/Bacteroidetes ratio (F/B ratio) was calculated as a biomarker of gut dysbiosis. E) Relative proportion of butyrate-, acetate- and lactate-producing bacteria expressed as relative abundance of total Bacteria. F) Relative proportion of strict anaerobic and aerobic bacteria in the gut microbiota in Wistar Kyoto rats (WKY), untreated SHR and SHR treated with SPIR (SHR-SPIR). Values are expressed as mean ± SEM (n = 8). *P < 0.05 significant differences compared with Wistar Kyoto rats (WKY). #P < 0.05 significant differences compared with untreated SHR group.

3. Results

3.1. Spironolactone decreases BP, improving the vascular nitric oxide (NO) pathway, and reducing oxidative stress and Th17 infiltration in aorta

As shown in Fig. 1A, B the SHR had a significant increase in the SBP and HR compared with the WKY rats (213.5 ± 6.4 mmHg and 416.9 ±

8.6 bpm vs. 154.2 ± 3.5 mmHg and 383.9 ± 5.7 bpm). The five-week spironolactone treatment induced a progressive reduction in both parameters reaching a total reduction in SHR of 37.5 ± 3.4 mmHg and 30.9 ± 7.1 bpm, respectively. In addition, increased heart weight/tibia length (HW/TL), left ventricle weight/tibia length (LVW/TL) and kidney weight/tibia length (KW/TL) ratios were observed in the SHR compared with those in the WKY groups. Chronic spironolactone significantly reduced left ventricular hypertrophy in SHR (Fig. 1C).

Table 1

Effect of spironolactone (SPIR) on phyla proportion of gut microbiota from spontaneously hypertensive rats (SHR).

	WKY (n = 8)	SHR (n = 8)	P value (SHR vs WKY)	SHR+SPIR (n = 8)	P value (vs SHR)
Actinobacteria	0.16 ± 0.03	0.56 ± 0.19	0.043	0.07 ± 0.02	0.017
Bacteroidetes	37.96 ± 5.25	24.80 ± 3.01	0.036	38.52 ± 4.74	0.021
Firmicutes	56.61 ± 4.95	71.22 ± 2.58	0.014	55.82 ± 4.36	0.006
Verrucomicrobia	0.92 ± 0.19	1.71 ± 0.49	0.135	2.28 ± 0.67	0.473
Proteobacteria	0.04 ± 0.01	0.08 ± 0.02	0.118	0.35 ± 0.19	0.157
Tenericutes	0.01 ± 0.01	0.41 ± 0.23	0.084	0.37 ± 0.11	0.892
Cyanobacteria	0.01 ± 0.01	0.01 ± 0.01	0.362	0.01 ± 0.01	0.362
Others	4.31 ± 2.67	1.23 ± 0.42	0.244	2.59 ± 0.67	0.088

The aortic concentration-contractile response curves to phenylephrine were similar among all groups (Fig. 2A). However, aortae from SHR displayed significatively decreased endothelium-dependent vasodilator responses to acetylcholine compared to WKY (~ - 38 % area under curve, AUC) (Fig. 2B), which were improved by spironolactone by ~ 48 %. After the incubation with L-NAME in the organ bath the acetylcholine-induced relaxation was abolished for all groups, pointing to NO being involved in this relaxation (data not shown). VAS2870 improved the relaxation response to acetylcholine in SHR group to WKY values, suggesting the involvement of NADPH oxidase activity in the impaired relaxation to acetylcholine in SHR (Fig. 2C). Moreover, the NADPH oxidase activity increased (~ 68 %) in SHR group as compared to WKY and normalized after spironolactone (Fig. 2D).

Vascular T cell infiltration seems to regulate ROS production and endothelial function in SHR [2,7]. Increased T helper (Th)17 and Th1 cells and decreased Tregs infiltration was detected in aorta from SHR, as compared to WKY. Chronic spironolactone normalized Th17 cells infiltration in SHR, being without effects in regulatory T cells (Tregs) and Th1 content (Fig. 2E).

3.2. Spironolactone treatment reduces gut dysbiosis in SHR

Given the key role of the gut microbiota in SHR [3–6] we examined the effects of spironolactone on the shifts in gut microbiota. Alpha diversity of gut bacterial communities was analysed by calculating two relevant ecological parameters: Chao richness and Shannon diversity. No significant changes were observed among the three groups in alpha diversity parameters (Fig. 3A). The axonometric two-dimensional PCoA at genus level showed WKY and SHRs to be significantly different (Fig. 3B) as described in other experiments [3,5–8,12] representing 2 distinct gut microbial communities. Spironolactone treatment changed effectively the composition of gut microbiota communities in SHR approaching near WKY (Fig. 3B). Percentages for the phyla Firmicutes and Actinobacteria were increased in SHR, meanwhile Bacteroidetes was lower, compared to WKY. Spironolactone treatment restored bacteria from these phyla to WKY-like proportions (Table 1, Fig. 3C). The Firmicutes/Bacteroidetes (F/B) ratio is broadly seen as an indicator of gut dysbiosis [3] and it was ~1.8-fold elevated for SHR, being normalized by spironolactone treatment (Fig. 3D). The dysbiosis of gut microbiota in SHR is characterized by changes in SCFAs-producing bacteria populations [3,5–8,12]. In our experiment there was a decrease in the proportions of acetate-producing bacteria, with no significant differences present in the populations of butyrate- and lactate-producing bacteria between SHR and WKY (Fig. 3E). Spironolactone treatment restored the level of acetate-producing bacteria

(specially the changes in the *Bacteroides, Bacteroidaceae, Bacteroidales*; and *Prevotella, Prevotellaceae, Bacteroidales*, Fig. S1, S2) and it was able to reduce the butyrate-producing bacteria (specially the changes in the *Eubacterium, Eubacteriaceae, Clostridiales*, Fig. S1, S2). Moreover, the populations of strict aerobic bacteria were increased in SHR compared with WKY, but no significant differences in strict anaerobic bacteria were detected. Spironolactone was able to restore these changes in aerobic populations (Fig. 3F).

3.3. Spironolactone improves gut pathology, inflammation, permeability, α-defensins production, and changes MLNs T cells in SHR

Hypertension has been linked to a reduction in gut tight junction proteins levels, and an increase in gut permeability and gut pathology [10]. In the colon, the SHR showed thickening of the muscle layer, an increase in the connective tissue area, and a decrease in villi length compared with those in the WKY group (Fig. 4A). Additionally, a reduced percentage of goblet cells (Fig. 4B) and an increase in thickness of adventitia and the amount of connective tissue around arterioles (Fig. 4C) were also observed in the colon of the SHR compared with those in the WKY group. Chronic spironolactone treatment reduced the connective tissue and the thickness of the muscle layer and increased the villi length in the colon of the SHR, being without significant effect in the goblet cells proportion. Interestingly, the higher crossectional area of colonic arterioles found in SHR as compared with WKY were reduced in SHR-SPIR. Next, we also examined the mRNA levels of proinflammatory cytokines in colon. The higher mRNA concentrations of IL-1ß, and TNF-α in SHR than WKY were normalized by spironolactone (Fig. S3).

We also investigated the effects of spironolactone on gut integrity in the colon by measuring tight junction proteins (ZO-1 and occludin) and mucins (MUC) levels. Lower mRNA levels and protein for ZO-1 and occludin were detected in colon from SHR compared to WKY (Fig. 5A). Spironolactone treatment increased occludin expression in colon, suggesting a recuperation of barrier function. Also, an increased gut permeability in adult hypertensive SHR was linked to decreased numbers of goblet cells [23], which function is to excrete mucins, protecting the gut from pathogen invasion, and regulating the gut immune response [28]. MUC-2 transcripts were detected downregulated too in the SHR group, which was unaffected by spironolactone. Similarly, reduced mRNA levels of MUC-3 in SHR were found, but spironolactone restored its gene expression (Fig. 5B), lowering gut permeability in SHR-SPIR group. Plasma endotoxin levels were higher in SHR compared with WKY group and were unaltered by the spironolactone treatment (Fig. 5C). Our results point to higher intestinal permeability in SHR that could facilitate the migration bacterial components (e.g., LPS) to the blood stream. I-FABP is a known marker of gut permeability [29], and mounting evidence has shown higher circulating I-FABP in animals and human with hypertension [29,30]. We detected increased plasma I-FABP in the SHR group compared with those in WKY animals. Remarkably, spironolactone was able to reduce I-FABP plasma levels (Fig. 5D).

Epithelial intestinal cells can synthesise α-defensins, cysteine-rich cationic peptides with antibiotic activity against microorganisms [31], to balance the composition of intestinal microbiota [32]. Our experiment in SHR shows a reduction in the α-defensin rat neutrophil peptide (RNP)1–2 expression levels, and high mRNA levels of RNP3 and RNP4 in colon in comparison with the WKY group. Spironolactone restored defensin levels to WKY group levels (Fig. 6).

As reported in the past, bacteria can translocate through the intestinal barrier, activating macrophages and dendritic cells that migrate to lymph nodes in the lower intestinal tract in altered gut mucosal integrity conditions [33]. These CX3CR1 + cells can process antigens for their presentation to naïve CD4 + T cells, activating T cell proliferation. We have observed that the percentage of Th17 and Th1 lymphocytes was higher in MLNs from SHR compared with WKY group, whereas Tregs were decreased in SHR (Fig. 7A). Spironolactone treatment normalized
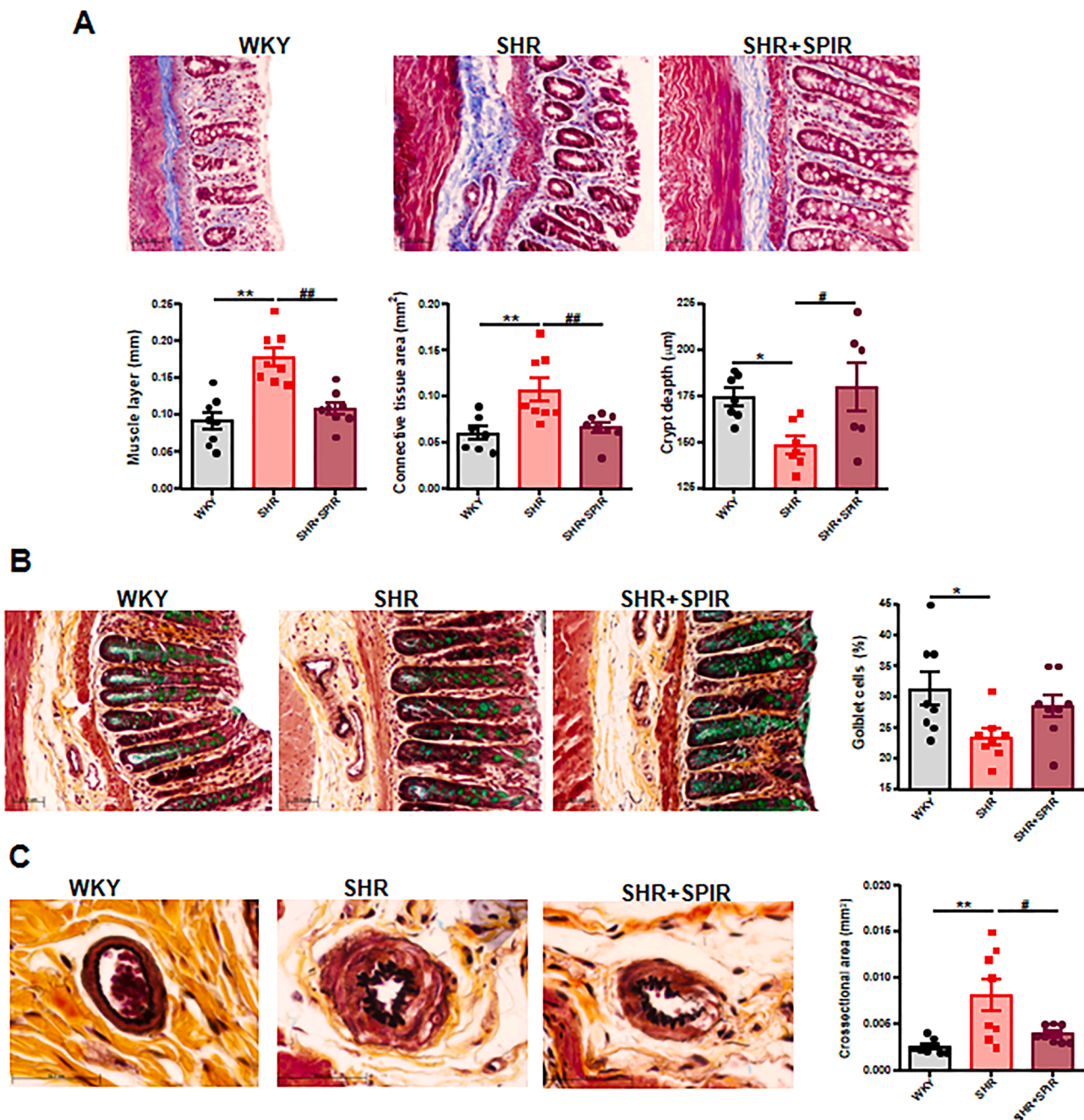
Fig. 4. Spironolactone (SPIR) improves the gut pathological alterations in the colon in spontaneously hypertensive rats (SHR). A) Representative micrographs of Masson-trichrome staining and quantitative analysis of muscle layer length, connective tissue area, and crypt depth in the colon in all experimental groups. B) Representative micrographs of Movat's pentachromic (MP) staining and quantitative analysis of number of goblet cells per 100 epithelial cells in the colon in all experimental groups. C) Representative micrographs of MP staining and quantitative analysis of the area of the submucosal vascular smooth muscle layer in vessels less than 70 µm of the colon in all experimental groups. Bar scale: 50 µm. Values are expressed as mean ± SEM (n = 8). *P < 0.05 and * *P < 0.01 significant differences compared with Wistar Kyoto rats (WKY). #P < 0.05 and ##P < 0.01 significant differences compared with untreated SHR group.

Th17 proportion in MLNs from SHR but did not change neither Tregs nor Th1 content. Similar data were found in blood from all experimental groups (Fig. 7B).

3.4. Spironolactone did not protect against neuroinflammation, but decreased gut sympathetic tone in the SHR

Increased neuroinflammation and oxidative stress within autonomic brain regions have been linked to hypertension [9]. MR activation in the hypothalamus leads to salt sensitivity acquisition and increased sympathetic activity [34]. We analyzed the effects of MR blockade with spironolactone in neuroinflammation, oxidative stress and sympathetic activity. We found that the mRNA levels of pro-inflammatory cytokines TNF-α, IL-1ß, and IL-6 (Fig. 8A) in brain PVN (one key autonomic brain region controlling BP) were increased in SHR compared to WKY, and unaltered by spironolactone. TLR4 activation within the brainstem contributes to neuroinflammation and the enhanced sympathetic outflow [22]. TLR4 mRNA levels in PVN from SHR group were higher than WKY group and were unaltered by spironolactone (Fig. 8B). Increased oxidative stress in PVN derived from activated NADPH oxidase is responsible for increasing central sympathetic outflow [35]. ROS production (Fig. 8C), NADPH oxidase activity (Fig. 8D) and the mRNA
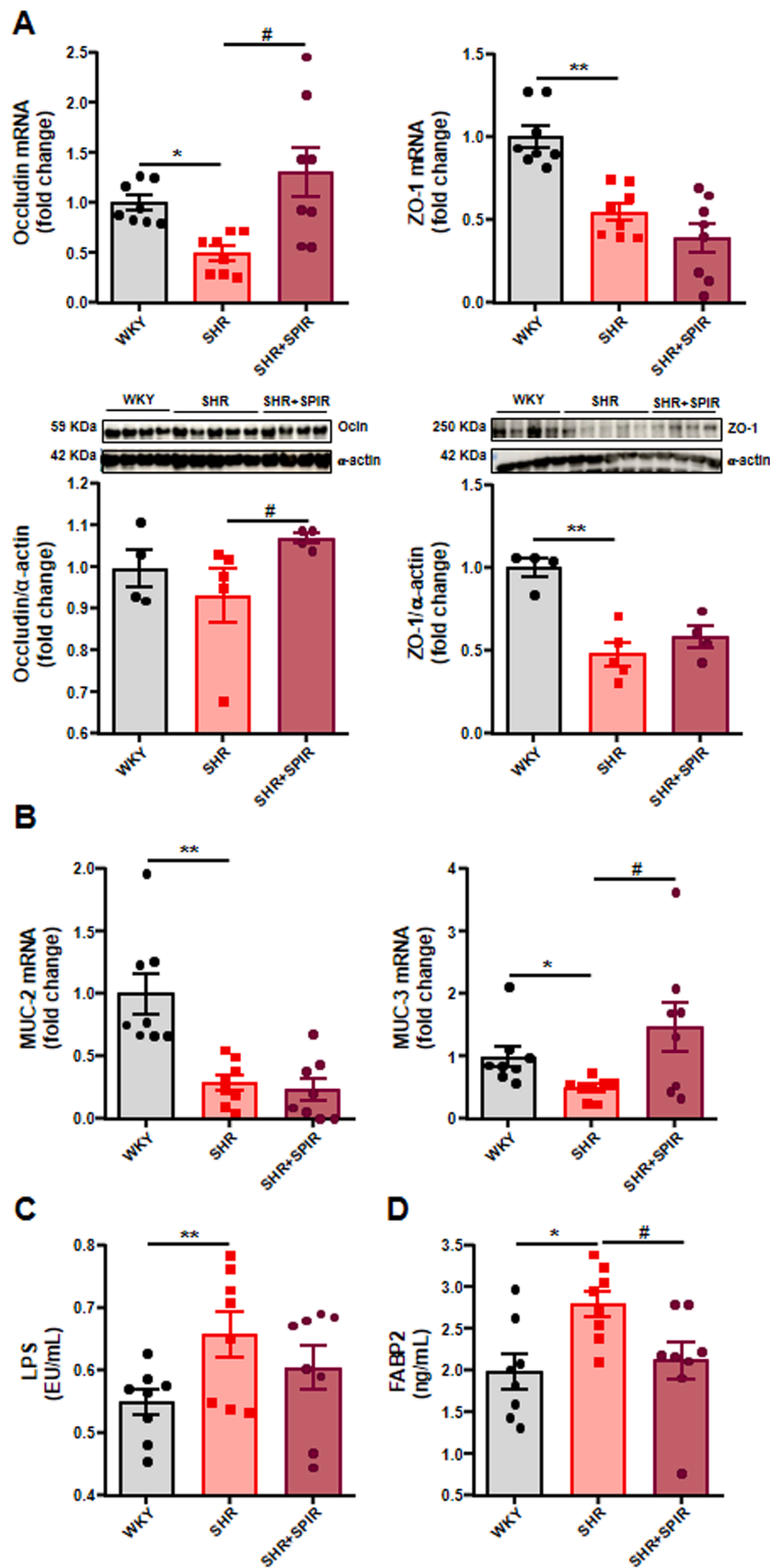
Fig. 5. Spironolactone (SPIR) induces an improvement in gut integrity and permeability in spontaneously hypertensive rats (SHR). A) mRNA levels and protein of occludin, and zonula occludens-1 (ZO-1) in the colon in all experimental groups. B) mRNA levels of mucin (MUC)− 2, and MUC-3 in the colon in all experimental groups. C) Levels of plasma endotoxin (endotoxin units/mL (EU/mL). D) Measurement of intestinal FABP level in the plasma. Values are expressed as mean ± SEM (n = 8). *P < 0.05 and **P < 0.01 significant differences compared with Wistar Kyoto rats (WKY). #P < 0.05 and ##P < 0.01 significant differences compared with untreated SHR group.
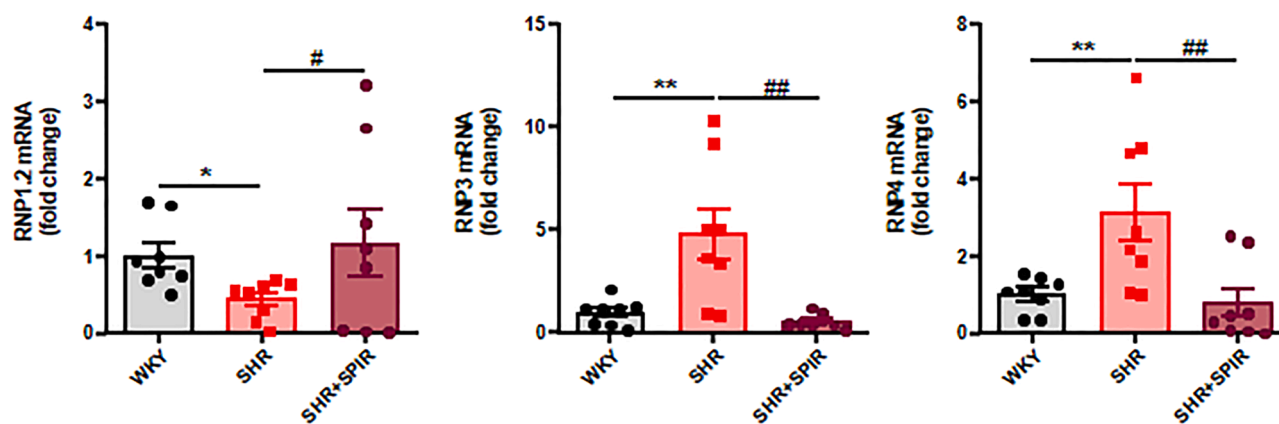
Fig. 6. Spironolactone (SPIR) induces an improvement in α-defensins production in spontaneously hypertensive rats (SHR). mRNA levels of α-defensins (RNP1.2, RNP3, and RNP4) in colon from Wistar Kyoto rats (WKY), untreated SHR (SHR) and SHR treated with SPIR (SHR+SPIR). Values are expressed as mean ± SEM (n = 8). *P < 0.05 and * *P < 0.01 significant differences compared with WKY. #P < 0.05 and ##P < 0.01 significant differences compared with untreated SHR group.

levels of NADPH oxidase subunits, NOX4, p22phox, and p47phox (Fig. 8E) were observed higher in SHR group than WKY group. However, spironolactone was also unable to reduce all these parameters. To stablish the effects of spironolactone in sympathetic outflow, we measured plasma NA concentration. Plasma NA concentration was higher in SHR as compared with WKY, which were reduced by spironolactone (Fig. 8F), showing reduced sympathetic activity. The increased sympathetic activity to the gut causes alterations in gut junction proteins in SHR [23]. Higher levels of tyrosine hydroxylase (TH) were detected, a crucial enzyme for the generation of NA, and NA content in the colon from SHR compared to WKY group, effects abolished by spironolactone (Fig. 8G). These results suggest that a reduction in intestinal sympathetic tone could be linked to the positive effects of spironolactone.

4. Discussion

A key element found in our experiment is that antihypertensive effects induced by chronic blockade of MR with spironolactone is associated with improvement of gut dysbiosis in SHR. Evidences for this are the following: 1) attenuation of gut wall pathology and leakiness; (ii) reshaping of colonic α-defensins production; (iii) repopulation with bacterial communities linked with normal BP; (iv) attenuation of Th17 population in MLNs, blood, and aorta; and (v) dampened sympathetic activity. Thus, beneficial effects of spironolactone could, in part, be due to its influence on the gut-vascular wall axis.

The link between gut dysbiosis, immune system and hypertension has already been discussed multiple times [5,7,12]. The conclusion to our experiment is consistent with what has already been stablished [15–17,36], MR blockade inducing lower BP in SHR. Plus, spironolactone restored the endothelial function joined to a decreased ROS production as reported previously [16,17]. A link between gut dysbiosis and hypertension has been confirmed in patients and animal models with hypertension, such as SHR. Mounting evidence points to gut microbiota and gut-vascular wall communication being crucial in hypertension [5]. In addition, intestinal microbiota composition has value in predicting major adverse cardiovascular and cerebrovascular events in patients with refractory hypertension [38], the main clinical target of spironolactone. Recent articles detail how gut dysbiosis is displayed in a broad range of experimental models of hypertension [3,5–8,11,12, 38–41]. The conclusions to this experiment are partially in concordance with the key known characteristics of dysbiotic microbiota seen elsewhere in SHR [3,5–8,11,12,41], such as, a high F/B ratio, a reduction in acetate-producing bacteria and an increase in strict aerobic bacteria. Spironolactone tended to the normalization of gut microbiota, reducing

the F/B ratio, normalizing SCFAs-producing microorganisms (increasing the acetate-producing bacteria *Prevotella*) and reducing strict aerobic bacteria population. Lower *Prevotella* abundance in feces is a hallmark of cardiovascular events in patients with refractory hypertension [37]. Acetate produced by bacteria could be involved in the antihypertensive effects of spironolactone. In fact, acetate consumption prevented the development of hypertension and endothelial dysfunction in a deoxycorticosterone acetate-salt murine model of hypertension [38,40] and in SHR [41]. Different authors have reported the ability of certain SCFA, like acetate, to modulate the immune response [42]. We found an expansion in acetate-producing bacteria in SHR-SPIR, which might be involved in the lower numbers of Th17 found in MLN and aorta from SHR-SPIR. Surprisingly, spironolactone could not increase Tregs population in MLNs, which would be related with the lower abundance of butyrate-producing bacteria, being butyrate the main microbial metabolite that regulates Treg differentiation [43].

Several explanations by which spironolactone could induce changes in gut microbiota were observed. Changes in the host health status are complemented by changes in gut microbiota populations. Consequently, the microbiota could be modulated to decrease BP, changing to compositions like those found in normotensive rats. However, we have already shown that hydralazine can normalize BP in SHR but remains unable to improve dysbiosis [12], discarding the possibility that gut microbiota adapted to normotensive conditions. Changes in gut microbiota populations have been associated with gut integrity [12,30]. Our results demonstrate pathological changes in the gut of hypertensive animals. This includes increased permeability and leakiness, fibrosis, and muscular tissues in the gut wall. In addition, stunted villi and decreased goblet cells were observed in SHR. The mammalian digestive tract epithelial cells create a tight barrier in the gut, contributing to the hypoxic environment of the lumen. Damage to this barrier makes the environment less hypoxic, conducive to aerobic bacterial growth [44]. In the SHR was found a reduction in the expression of tight junction proteins, being occludin normalized by the spironolactone. Moreover, increased intestinal permeability in adult hypertensive SHR has been related to reduced goblet cells, and mucins [23]. Spironolactone tended to increase colonic goblet cells and increased mRNA levels of MUC-3. These protective effects in gut integrity are associated with reduced plasma levels of FABP2, a marker of gut permeability. In addition, intestines of SHR were significantly less hypoxic and presented increased aerobic bacteria in feces, due to a reduction in the epithelium barrier integrity [12]. We also found a higher population of aerobic bacteria in feces from SHR, which were linked to a loss of gut integrity. Spironolactone increased colonic integrity and reduced the populations of strict aerobic bacteria. The data reinforces the essential role of gut
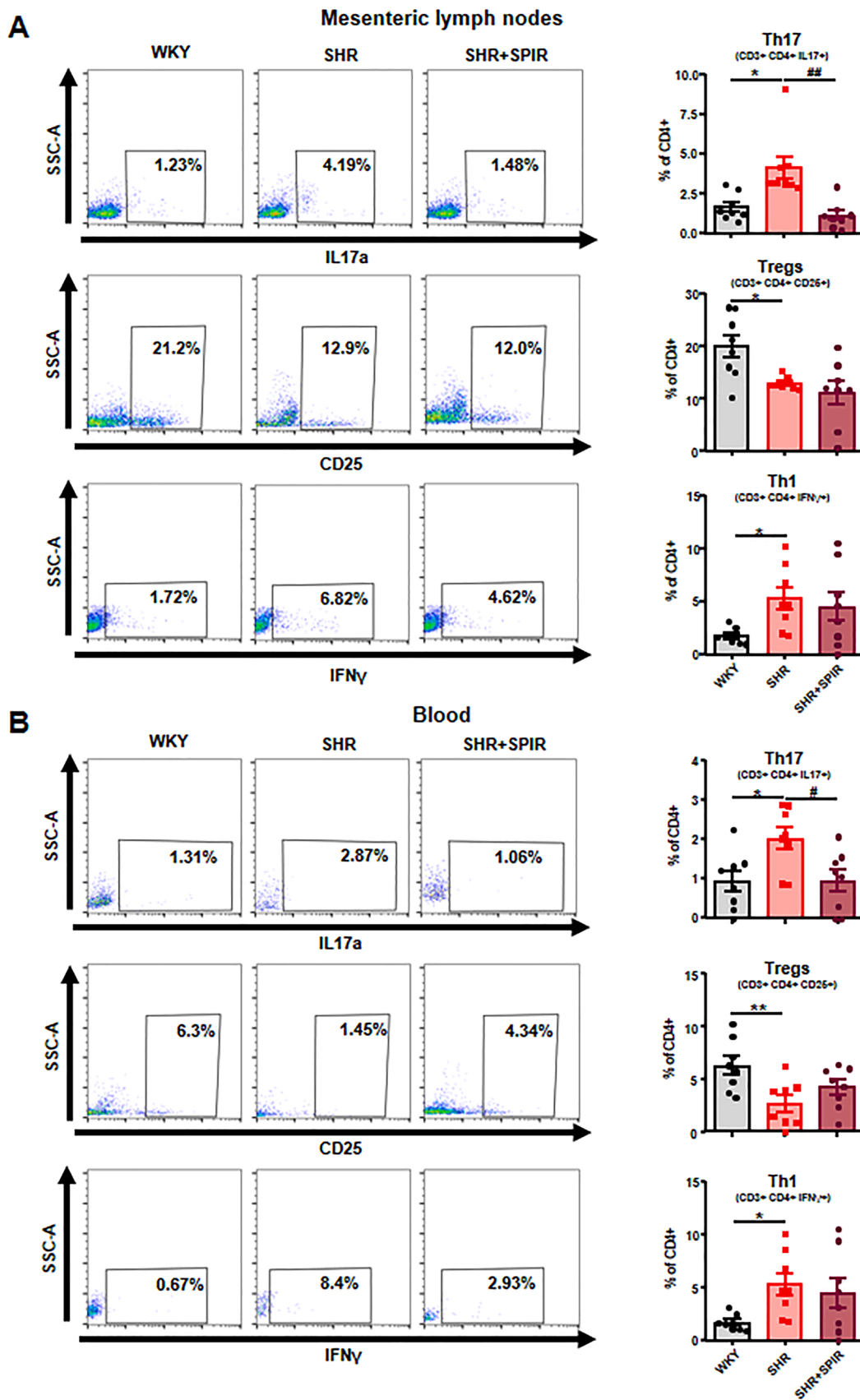
Fig. 7. Spironolactone (SPIR) improves T cell profile at Mesenteric lymph nodes (MLNs) and blood in spontaneously hypertensive rats (SHR). T helper (Th)− 17 (CD3 + CD4 + IL17a+), regulatory T cells (Treg; CD3 + CD4 + CD25 +), and Th1 (CD3 + CD4 + IFNγ+) measured by flow cytometry in MLNs (A) and blood (B) from all experimental groups. Values are expressed as mean ± SEM (n = 8). *P < 0.05 and * *P < 0.01 significant differences compared with Wistar Kyoto rats (WKY). #P < 0.05 and ##P < 0.01 significant differences compared with untreated SHR group.
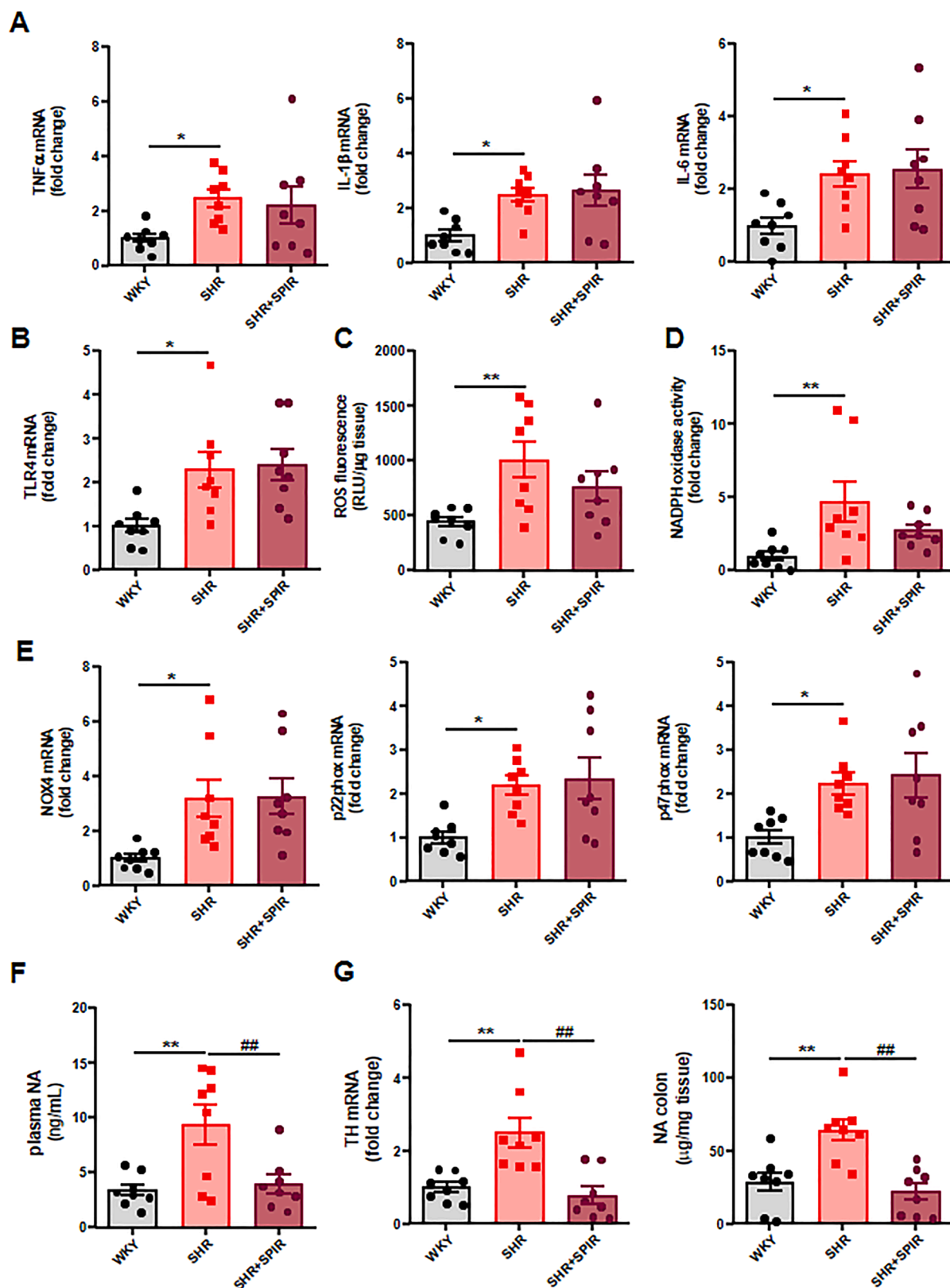
Fig. 8. Spironolactone (SPIR) cannot reduce neuroinflammation, and ROS production in the paraventricular nucleus (PVN) of the hypothalamus in spontaneously hypertensive rats (SHR) but reduces the sympathetic tone. mRNA levels of pro-inflammatory cytokines, tumor necrosis factor α (TNFα), interleukin (IL)− 1β, and IL6 (A), and toll like receptor (TLR)− 4 (B) in homogenates from brain PVN. C) CM-H2DCFDA-detected intracellular ROS and NADPH oxidase activity (D) measured by DHE fluorescence in the microplate reader in homogenates from brain PVN. E) mRNA levels of NADPH oxidase subunits NOX4, p22phox, and p47phox in PVN. F) Plasma noradrenaline (NA) content from all experimental groups. G) Colonic tyrosine hydroxylase (TH) expression and colonic NA concentration. Values are expressed as mean ± SEM (n = 8). *P < 0.05 and * *P < 0.01 significant differences compared with Wistar Kyoto rats (WKY). ##P < 0.01 significant differences compared with untreated SHR group.

integrity in the composition of intestinal microbiota. Furthermore, intestinal epithelial cells and Paneth cells secrete antimicrobial peptides, such as defensins, which selectively kill Gram-positive bacteria [45–48]. We detected changes in defensin levels in colon from SHR compared to WKY, which might also be involved in changes in SHR microbiota, which were normalized by spironolactone treatment, and might contribute to reshaping of gut microbiota. Our present data agree with Santisteban et al., [23], pointing to an increased gut sympathetic drive (higher TH levels and NA content) associated with microbial dysbiosis and reduced gut integrity in hypertensive animals.

Resistant hypertension is primarily of neurogenic origin, exhibiting higher sympathetic activity. Past experiments have suggested that an activated microglia-neuron unit in the PVN increases gut sympathetic drive; linked to an increased gut pathology and inflammatory status, and altered gut microbiota and permeability, showing a brain-gut axis driven by a sympathetic response [6,9,23,49]. In fact, inhibition of neuroinflammation by intracerebroventricular administration of a modified tetracycline normalizes the sympathetic activity, inducing changes in microbiota populations and the amelioration of gut pathology [9]. Moreover, activation of PVN AT1 receptor triggers the sympathetic outflow stimulating NADPH oxidase-dependent ROS production [35]. In agreement with these data, we observed in PVN from SHR a higher NADPH oxidase-driven ROS production, and a higher pro-inflammatory cytokine (TNF-α, IL-1β, and IL-6) expression than WKY group. Unexpectedly, spironolactone was unable to reduce neuroinflammation and ROS production in PVN but reduced sympathetic excitation (lower plasma NA levels). The change in sympathetic activity induced by spironolactone seems to be independent of changes in TLR4 pathway in PVN. This reduced sympathetic drive would be related to the reduced cerebrospinal fluid Na^+ concentration because of MR/epithelial Na channels pathway blockade in choroid plexus, as described previously by eplerenone in hypertensive rats [50]. However, further studies are needed to explore this mechanism.

Previous studies demonstrated that reduction of sympathetic activity in the colon induced by captopril [23] or losartan [12] improved gut pathology and decreased gut dysbiosis parameters, while hydralazine (which increases gut sympathetic drive) was incapable of normalizing gut integrity and microbiota composition [12]. We detected higher mRNA levels of TH and NA content in SHR colon, which were restored by spironolactone. Thus, spironolactone in SHR reduces the sympathetic excitation, lending to lower gut sympathetic drive (lower colonic TH expression and NA content), improving gut pathology and gut dysbiosis in SHR.

In conclusion, we can assert that spironolactone improves gut dysbiosis in SHR. This appears to be associated with its ability to ameliorate gut integrity by reducing the intestinal sympathetic drive. Whether these beneficial effects in the gut contribute to the antihypertensive effects deserve further investigation.

Authors contribution

C.G.-C., J.M. and S.M. contributed equally as first authors. J.D. conceived and designed the research; C.G.-C., J.M., S.M., I.R.V, M.T., N. M.-M., F.O., M.S., M.G.G., and M.R. performed the experiments and analysed the data; R.J. and J.D. interpreted the results; C.G.-C., J.M., S. M., M.S., and R.J. prepared figures; M.R. and J.D. drafted this manuscript; I.R.V, M.T., M.G.G, M.R. and J.D. edited and revised the manuscript; All authors approved the final version of manuscript. M.R. and J. D. contributed equally to the supervision of the study as senior authors.

Conflict of interest statement

This study demonstrates for the first time that spironolactone reduces gut dysbiosis in SHR. This effect could be related to its capability to improve gut integrity and pathology due to reduced sympathetic drive in the gut.

Data Availability

Data will be made available on request.

CRediT authorship contribution statement

All authors have read and approved the submission of the manuscript; the manuscript has not been published and is not being considered for publication elsewhere, in whole or in part, in any language, except as an abstract.

Appendix A. Supporting information

Supplementary data associated with this article can be found in the online version at doi:10.1016/j.biopha.2022.114149.

References

[1] R.M. Touyz, F.J. Rios, R. Alves-Lopes, K.B. Neves, L.L. Camargo, A.C. Montezano, Oxidative stress: a unifying paradigm in hypertension, Can. J. Cardiol. 36 (5) (2020) 659–670, https://doi.org/10.1016/j.cjca.2020.02.081.

[2] T.J. Guzik, N.E. Hoch, K.A. Brown, L.A., et al., Role of the T cell in the genesis of angiotensin II induced hypertension and vascular dysfunction, J. Exp. Med 204 (10) (2007) 2449–2460, https://doi.org/10.1084/jem.20070657.

[3] T. Yang, M.M. Santisteban, V. Rodriguez, et al., Gut dysbiosis is linked to hypertension, Hypertension 65 (6) (2015) 1331–1340, https://doi.org/10.1161/HYPERTENSIONAHA.115.05315.

[4] J. Li, F. Zhao, Y. Wang, et al., Gut microbiota dysbiosis contributes to the development of hypertension, Microbiome 5 (1) (2017) 14, https://doi.org/10.1186/s40168-016-0222-x.

[5] M. Toral, I. Robles-Vera, N. de la Visitación, et al., Role of the immune system in vascular function and blood pressure control induced by faecal microbiota transplantation in rats, Acta Physiol. (Oxf.) 227 (1) (2019), e13285, https://doi.org/10.1111/apha.13285.

[6] M. Toral, I. Robles-Vera, N. de la Visitación, M, et al., Critical role of the interaction gut microbiota-sympathetic nervous system in the regulation of blood pressure, Front. Physiol. 10 (2019) 231, https://doi.org/10.3389/fphys.2019.0023.

[7] I. Robles-Vera, N. de la Visitación, M. Toral, et al., Mycophenolate mediated remodeling of gut microbiota and improvement of gut-brain axis in spontaneously hypertensive rats, Biomed. Pharmacother. 135 (2021), 1111189, https://doi.org/10.1016/j.biopha.2020.111189.

[8] W.J. Xia, M.L. Xu, X.J. Yu, et al., Antihypertensive effects of exercise involve reshaping of gut microbiota and improvement of gut-brain axis in spontaneously hypertensive rat, Gut Microbes 13 (1) (2021) 1–24, https://doi.org/10.1080/19490976.2020.1854642.

[9] R.K. Sharma, T. Yang, A.C. Oliveira, et al., Microglial cells impact gut microbiota and gut pathology in angiotensin ii-induced hypertension, Circ. Res. 124 (5) (2019) 727–736, https://doi.org/10.1161/CIRCRESAHA.118.313882.

[10] M.M. Santisteban, N. Ahmari, J.M. Carvajal, et al., Involvement of bone marrow cells and neuroinflammation in hypertension, Circ. Res 117 (2) (2015) 178–191, https://doi.org/10.1161/CIRCRESAHA.117.305853.

[11] T. Yang, V. Aquino, G.O. Lobaton, et al., Sustained captopril-induced reduction in blood pressure is associated with alterations in gut-brain axis in the spontaneously hypertensive rat, J. Am. Heart Assoc. 8 (4) (2019), e010721, https://doi.org/10.1161/JAHA.118.01072.

[12] I. Robles-Vera, M. Toral, N. de la Visitación, et al., Changes to the gut microbiota induced by losartan contributes to its antihypertensive effects, Br. J. Pharmacol. 177 (9) (2020) 2006–2023, https://doi.org/10.1111/bph.14965.

[13] P.J. Fuller, M.J. Young, Mechanisms of mineralocorticoid action, Hypertension 46 (6) (2005) 1227–1235, https://doi.org/10.1161/01.HYP.0000193502.77417.17.

[14] M.E. Brocca, L. Pietranera, M. Meyer, et al., Mineralocorticoid receptor associates with pro-inflammatory bias in the hippocampus of spontaneously hypertensive rats, J. Neuroendocrinol. 29 (7) (2017), https://doi.org/10.1111/jne.12489.

[15] D.H. Endemann, R.M. Touyz, C. Iglarz, C. Savoia, E.L. Schiffrin, Eplerenone prevents salt-induced vascular remodeling and cardiac fibrosis in stroke-prone spontaneously hypertensive rats, Hypertension 43 (6) (2004) 1252–1257, https://doi.org/10.1161/01.HYP.0000128031.31572.a3.

[16] D. Sanz-Rosa, M.P. Oubiña, E. Cediel, et al., Eplerenone reduces oxidative stress and enhances eNOS in SHR: vascular functional and structural consequences, Antioxid. Redox Signal. 7 (9–10) (2005) 1294–1301, https://doi.org/10.1089/ars.2005.7.1294.

[17] N. de las Heras, M. Ruiz-Ortega, M. Miana, et al., Interactions between aldosterone and connective tissue growth factor in vascular and renal damage in spontaneously hypertensive rats, J. Hypertens. 25 (3) (2007) 629–638, https://doi.org/10.1097/HJH.0b013e3280112ce5.

[18] M. Nishihara, Y. Hirooka, T. Kishi, K. Sunagawa, Different role of oxidative stress in paraventricular nucleus and rostral ventrolateral medulla in cardiovascular regulation in awake spontaneously hypertensive rats, J. Hypertens. 30 (2012) 1758–1765, https://doi.org/10.1097/HJH.0b013e32835613d7.

[19] J.C. McGrath, E. Lilley, Implementing guidelines on reporting research using animals (ARRIVE etc.): new requirements for publication in BJP, Br. J. Pharmacol. 172 (13) (2015) 3189–3193, https://doi.org/10.1111/bph.12955.

[20] L.M. Pereira, C.A. Mandarim-de-Lacerda, Myocardial changes after spironolactone in spontaneous hypertensive rats. A laser scanning confocal microscopy study, J. Cell. Mol. Med 6 (1) (2002) 49–57, https://doi.org/10.1111/j.1582-4934.2002.tb00310.x.

[21] R. Vera, R. Jiménez, F. Lodi, et al., Genistein restores caveolin-1 and AT-1 receptor expression and vascular function in large vessels of ovariectomized hypertensive rats, Menopause 14 (5) (2007) 933–940, https://doi.org/10.1097/GME.0b013e31802d9785.

[22] R.B. Dange, D. Agarwal, R. Teruyama, J. Francis, Toll-like receptor 4 inhibition within the paraventricular nucleus attenuates blood pressure and inflammatory response in a genetic model of hypertension, J. Neuroinflamm. 12 (1) (2015) 31, https://doi.org/10.1186/s12974-015-0242-7.

[23] M.M. Santisteban, Y. Qi, J. Zubcevic, et al., Hypertension-linked pathophysiological alterations in the gut, Circ. Res 120 (2) (2017) 312–323, https://doi.org/10.1161/CIRCRESAHA.116.309006.

[24] M. Gómez-Guzmán, R. Jiménez, M. Sánchez, et al., Chronic (-)-epicatechin improves vascular oxidative and inflammatory status but not hypertension in chronic nitric oxide-deficient rats, Br. J. Nutr. 106 (9) (2011) 1337–1348, https://doi.org/10.1017/S0007114511004314.

[25] M.J. Zarzuelo, R. Jiménez, P. Galindo, et al., Antihypertensive effects of peroxisome proliferator-activated receptor-β activation in spontaneously hypertensive rats, Hypertension 58 (4) (2011) 733–743, https://doi.org/10.1161/HYPERTENSIONAHA.111.174490.

[26] M. Romero, M. Toral, I. Robles-Vera, et al., Activation of peroxisome proliferator activator receptor β/δ improves endothelial dysfunction and protects kidney in murine lupus, Hypertension 69 (4) (2017) 641–650, https://doi.org/10.1161/HYPERTENSIONAHA.116.08655.

[27] J. Chong, P. Liu, G. Zhou, J. Xia, Using MicrobiomeAnalyst for comprehensive statistical, functional, and meta-analysis of microbiome data, Nat. Protoc. 15 (3) (2020) 799–821, https://doi.org/10.1038/s41596-019-0264-1.

[28] A.M. Mowat, W.W. Agace, Regional specialization within the intestinal immune system, Nat. Rev. Immunol. 14 (10) (2014) 667–685, https://doi.org/10.1038/nri3738.

[29] B.R. Stevens, R. Goel, K. Seungbum, et al., Increased human intestinal barrier permeability plasma biomarkers zonulin and FABP2 correlated with plasma LPS and altered gut microbiome in anxiety or depression, Gut 67 (8) (2018) 1555–1557, https://doi.org/10.1136/gutjnl-2017-314759.

[30] S. Kim, R. Goel, A. Kumar, et al., Imbalance of gut microbiome and intestinal epithelial barrier dysfunction in patients with high blood pressure, Clin. Sci. 132 (6) (2018) 701–718, https://doi.org/10.1042/CS20180087.

[31] C.L. Bevins, Events at the host-microbial interface of the gastrointestinal tract. V. Paneth cell alpha-defensins in intestinal host defense, Am. J. Physiol. Gastrointest. Liver Physiol. 289 (2) (2005) G173–G176, https://doi.org/10.1152/ajpgi.00079.2005.

[32] T. Hashimoto, T. Perlot, A. Rehman, et al., ACE2 links amino acid malnutrition to microbial ecology and intestinal inflammation, Nature 487 (7408) (2012) 477–481, https://doi.org/10.1038/nature11228.

[33] J.H. Niess, S. Brand, X. Gu, et al., CX3CR1-mediated dendritic cell access to the intestinal lumen and bacterial clearance, Science 307 (5707) (2005) 254–258, https://doi.org/10.1126/science.110290.

[34] K. Ito, Y. Hirooka, K. Sunagawa, Acquisition of brain Na sensitivity contributes to salt-induced sympathoexcitation and cardiac dysfunction in mice with pressure overload, Circ. Res. 104 (8) (2009) 1004–1011, https://doi.org/10.1161/CIRCRESAHA.108.188995.

[35] L. Gao, W. Wang, Y.L. Li, et al., Sympathoexcitation by central ANG II: roles for AT1 receptor upregulation and NAD(P)H oxidase in RVLM, Am. J. Physiol. Heart Circ. Physiol. 288 (5) (2005) H2271–H2279, https://doi.org/10.1152/ajpheart.00949.2004.

[36] S.S. Pereira, L. Carvalho, M.M. Costa, et al., Mineralocorticoid receptor antagonists eplerenone and spironolactone modify adrenal cortex morphology and physiology, Biomedicines 9 (4) (2021) 441, https://doi.org/10.3390/biomedicines9040441.

[37] J. Jiao, Y. Zhang, P. Han, S. Zhai, A preliminary study on the value of intestinal flora in predicting major adverse cardiovascular and cerebrovascular events in patients with refractory hypertension, Comput. Math. Methods Med. 2022 (2022), 7723105, https://doi.org/10.1155/2022/7723105.

[38] F.Z. Marques, E. Nelson, P.Y. Chu, et al., High-fiber diet and acetate supplementation change the gut microbiota and prevent the development of hypertension and heart failure in hypertensive mice, Circulation 135 (10) (2017) 964–977, https://doi.org/10.1161/CIRCULATIONAHA.116.024545.

[39] I. Robles-Vera, M. Toral, N. de la Visitación, et al., The probiotic lactobacillus fermentum prevents dysbiosis and vascular oxidative stress in rats with hypertension induced by chronic nitric oxide blockade, Mol. Nutr. Food Res. 62 (19) (2018), e1800298, https://doi.org/10.1002/mnfr.201800298.

[40] I. Robles-Vera, N. de la Visitación, M. Toral, et al., Probiotic bifidobacterium breve prevents DOCA-salt hypertension, FASEB J. 34 (10) (2020) 13626–13640, https://doi.org/10.1096/fj.202001532R.

[41] I. Robles-Vera, M. Toral, N. de la Visitación, et al., Probiotics prevent dysbiosis and the rise in blood pressure in genetic hypertension: role of short-chain fatty acids, Mol. Nutr. Food Res. 64 (6) (2020), e1900616, https://doi.org/10.1002/mnfr.201900616.

[42] D.M. Kaye, W. Shihata, H.A. Jama, et al., Deficiency of prebiotic fibre and insufficient signalling through gut metabolite sensing receptors leads to cardiovascular disease, Circulation 141 (17) (2020) 1393–1403, https://doi.org/10.1161/CIRCULATIONAHA.119.043081.

[43] A.M. Tyagi, M. Yu, T.M. Darby, et al., The microbial metabolite butyrate stimulates bone formation via t regulatory cell-mediated regulation of WNT10B expression, Immunity 49 (6) (2018), https://doi.org/10.1016/j.immuni.2018.10.013, 1116-1131.e7.

[44] Z.M. Earley, S. Akhtar, S.J. Green, et al., Burn injury alters the intestinal microbiome and increases gut permeability and bacterial translocation, PLoS One 10 (7) (2015), e0129996, https://doi.org/10.1371/journal.pone.0129996.

[45] T. Ayabe, D.P. Satchell, C.L. Wilson, W.C. Parks, M.E. Selsted, A.J. Ouellette, Secretion of microbicidal alpha-defensins by intestinal Paneth cells in response to bacteria, Nat. Immunol. 1 (2) (2000) 113–118, https://doi.org/10.1038/77783.

[46] P. Vora, A. Youdim, L.S. Thomas, et al., Beta-defensin-2 expression is regulated by TLR signaling in intestinal epithelial cells, J. Immunol. 173 (9) (2004) 5398–5405, https://doi.org/10.4049/jimmunol.173.9.5398.

[47] E.G. Pamer, Immune responses to commensal and environmental microbes, Nat. Immunol. 8 (11) (2007) 1173–1178, https://doi.org/10.1038/ni1526.

[48] S. Vaishnava, C.L. Behrendt, A.S. Ismail, L. Eckmann, L.V. Hooper, Paneth cells directly sense gut commensals and maintain homeostasis at the intestinal host-microbial interface, Proc. Natl. Acad. Sci. USA 105 (52) (2008) 20858–20863, https://doi.org/10.1073/pnas.0808723105.

[49] J. Zubcevic, E.M. Richards, T. Yang, et al., Impaired autonomic nervous system-microbiome circuit in hypertension, Circ. Res. 125 (1) (2019) 104–116, https://doi.org/10.1161/CIRCRESAHA.119.313965.

[50] M. Nakano, T. Hirooka, R. Matsukawa, K. Ito, K. Sunagawa, Mineralocorticoid receptors/epithelial Na(+) channels in the choroid plexus are involved in hypertensive mechanisms in stroke-prone spontaneously hypertensive rats, Hypertens. Res. 36 (3) (2013) 277–284, https://doi.org/10.1038/hr.2012.174.